TRACKING OF RRR VALUE AND MICROSTRUCTURE IN HIGH PURITY NIOBIUM ALONG THE PRODUCTION CHAIN FROM THE INGOT TO THE FINISHED CAVITY

D. Janda, M. Heilmaier, TU Darmstadt, Germany
X. Singer, W. Singer, DESY, Germany
W. Simader, R. Grill, Plansee, Germany
F. Schölz, S. Grawunder, B. Spaniol, W.C. Heraeus, Germany

Abstract

The different influences on the RRR value, mainly grain-structure, grain orientation, tantalum contribution, amount of interstitial impurities are analysed.

INTRODUCTION

The residual resistivity ratio is a common indicator of the level of purity. *RRR* values indicate material purity with high sensitivity.

The RRR-value is defined as follows:

$$RRR = \frac{\rho(295K)}{\rho(4{,}2K)} \quad (1)$$

where ρ is the electrical resistivity at given temperature.

In one of the chain of sheet fabrication started from high purity niobium ingot an unexpectedly high scatter of RRR-values has been observed. Investigations to clarify the specific reasons for the observed scatter of RRR-values like hot gas extraction, EBSD (Electron backscattered diffraction) and EPMA (Electron probe micro analyzer) have been applied.

These investigations were carried out exemplarily on samples taken from sheet-material.

THEORETICAL AND METHODOLOGICAL APPROACH

It is well known that the electrical resistivity of metals at temperatures close to T=0 K is mainly caused by impurities ρ_{fa}, defects ρ_d and for thin specimens by electron-surface-scattering ρ_s. At this temperature the intrinsic resistivity from electron-phonon scattering $\rho_i(T)$ is negligible, but it becomes dominant at room temperature. Hence,

$$\rho = \rho_i(T) + \rho_{fa} + \rho_d + \rho_s \quad (2)$$

The used proportionality constants for calculation of the impurity effect ρ_{fa} per atomic percent are for oxygen (4.5), nitrogen (5.2) and tantalum (0.25) $\cdot 10^{-10}$ ohm·cm / at. ppm, respectively.

The main interstitially dissolved impurities, oxygen, nitrogen and hydrogen (O, N, H), act as scattering centers for unpaired electrons and reduce the RRR. Among the substitutionally dissolved metallic impurities, tantalum has the highest concentration. This element accompanies niobium in most ores. Tantalum and niobium are chemically akin; the separation of these elements occurs at the industry mostly by liquid-liquid extraction.

The maximum theoretical RRR-value can be calculated by assuming that only electron-phonon scattering $\rho_i(T)$ is present in equation 2. With $\rho_i(295\ K) = 14.58 \cdot 10^{-6}$ and $\rho_i(4{,}2\ K) = 4.5 \cdot 10^{-10}$ ohm·cm [3] the RRR_{max} will be

$$RRR_{max} = \frac{\rho_i(295K)}{\rho_i(4{,}2K)} = 32400 \quad (3)$$

The common and most important impurities have been measured on samples by hot gas extraction (interstitials) and mass spectroscopy using inductively coupled plasma (MS-ICP, tantalum).. Comparison between the measurements and the RRR calculations using equation 2 can give the hint, whether the major influences on the electrical conductivity have been considered correctly.

Furthermore, the quality of the sheet material for high gradient cavities does not only depend on the absolute concentration of impurities but also on their distribution [4].

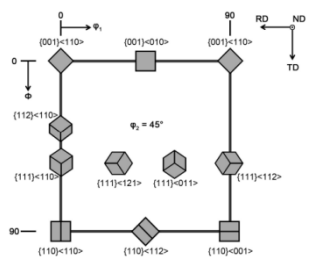

Figure 1: a) Cross section at φ_2= 45 with essential textures [6].

Rolling and annealing of metal sheets leads to distinct crystallographic textures. Figure 1 shows an example for an ideal fibre structure of body centered cubic (bcc) metals. It has been investigated, whether the evolved textures in the sheet material may have an influence on the RRR-value. The textures have been analyzed in the scanning electron microscope (SEM) utilizing EBSD (Electron backscattered diffraction).

RESULTS AND DISCUSSION

For the sake of simplicity, in the calculations of RRR-values only the influence of oxygen, nitrogen and tantalum has been taken into consideration. Comparison of measured and calculated RRR values for specimens A,B,C taken from niobium sheets shows that this is only the case for specimens A and B.

Table 1: Comparison of measured and calculated RRR-values

	Concentration (wt. ppm)			RRR (4,2 K)	
	Oxygen	Nitrogen	Tantalum	Measured	Calculated
Specimen A	11	2	150	264	380
	9	3			399
Specimen B	6	4	5	414	482
	6	4			482
Specimen C	13	2	150	430	334
	15	4			261

EPMA method was used for analysis of tantalum contents in the samples. Tantalum is homogeneously distributed in all three specimens. The absolute concentration and distribution of tantalum in specimens A and C is basically identical. A mean value of 150 µg/g was found for both specimens. This is shown by using the example of specimen A.

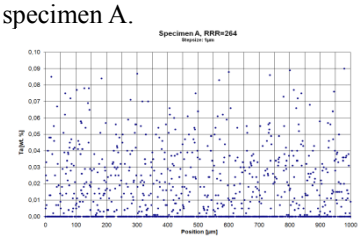

Figure 2: EPMA of specimen A

By comparison, specimen B shows hardly any tantalum.

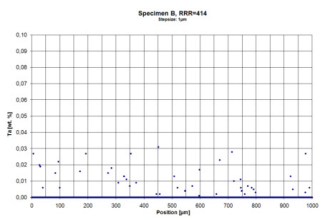

Figure 3: EPMA of specimen B

Earlier work showed already the appearance of pronounced textures occurred after cold rolling and annealing [7]. The {111} γ-fiber dominates in the center of the sheet, but the {100} cubic-texture dominates on the surface. Our investigations show the same characteristics. The specimen geometry and dominant textures in the related areas are illustrated in Figure 4.

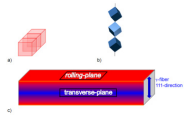

Figure 4: a) cubic-texture in the surface layer. b) γ-fiber in the center of layer. c) Specimen geometry and dominant textures.

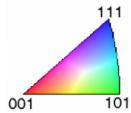

Figure 5: color-code for IPF pictures

Specimen A possesses a very dominant cubic-texture in the rolling plane (Figure .a). The related ODF cross section at φ_2=45° (Figure .b) indicates that the crystal lattice is oriented to the sheet geometry as displayed in Figure 4a and c. By inspecting the transverse-plane ODF of specimen A (Figure 7.b) the cubic-texture is shifted to 45° in the rolling plane. This indicates that the cubic texture from the edge toward the center of the transverse plane makes a shift of 45° until only the γ-fiber is prominent in the middle of the transverse plane. Specimens B and C show generally the same tendencies in the textures. Due to the longer etching times, the cubic-textures are not as dominant as in specimen A. In the rolling-plane of specimen B (Figure 9) the cubic-texture is already shifted 45°, like in the transversal-plane of specimen A. In specimen C (Figure 10) the cubic texture in the rolling-plane is completely removed and the γ-fiber becomes very dominant. The γ-fiber is dominant in the center of the transversal-planes of all three specimens.

a) b)

Figure 6: a) IPF of specimen A in the rolling plane; b) Including ODF cross section at φ_2=45°

a) b)

Figure 7: a) IPF of specimen A in the transverse plane; b) Including ODF cross section at φ_2=45°

a) b)

Figure 8: a) IPF of specimen B in the rolling plane; b) Including ODF cross section at φ_2=45°

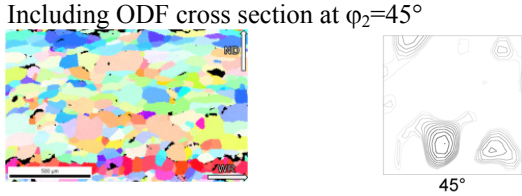

a) b)

Figure 9: a) IPF of specimen B in the transverse plane; b) Including ODF cross section at φ_2=45°

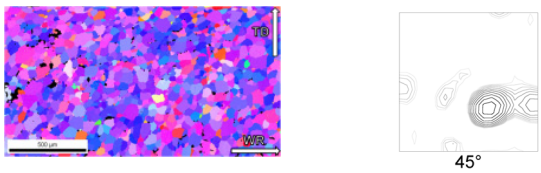

a) b)

Figure 10: a) IPF of specimen C in the rolling plane; b) Including ODF cross section at φ_2=45°

a) b)

Figure 11: a) IPF of specimen C in the transverse plane; b) Including ODF cross section at φ_2=45°

Relation between the RRR values and the orientation of the grains could not be observed.

Table 2: Comparison of RRR-value, grain size and fraction of high-angle grain boundaries

	Specimen A			Specimen B		Specimen C	
	Upside	underside	Center	Upside	Center	Upside	Center
RRR-value in respective area (4,2 K)	264	262	268	421	407	423	441
Grainsize (diameter) [µm]	59	62	80	57	117	66	104
High-angle grain-boundaries (>15°) [%]	32	62	40	68	50	60	54

Grain boundaries should not be a dominant factor, as they are almost equal in specimens A and B. Likewise, it is improbable that dislocations are responsible for the drop of the RRR-value, because significant differences in dislocation density would have been detected in the EBSD-measurements. However, generally dislocations may be responsible for large drops in the RRR-value. It is, thus, concluded that a complete recrystallization after rolling is essential to achieve high RRR-values.

In the RRR calculation we have not considered contributions from other impurities. The most likely reasons for measured and calculated RRR deviation are assumed to be unconsidered impurities (e.g. H or C) or not homogeneous distribution of interstitial impurities within of the sample that hardly can be detected.

CONCLUSIONS

The comparison of our theoretical calculations with the experimental research clearly yields the following results:

1) The nonhomogeneous distribution of Ta cannot be the reason of RRR scatter. In the areas investigated by EPMA tantalum is distributed homogeneously in all specimens.
2) Grain size and the fraction of high-angle grain boundaries (>15°) have a negligible effect on the RRR-value in the reviewed RRR-array.
3) No influence of the observed textures on the RRR-value could be established. The scatter of RRR-values could be probably caused by nonhomogeneous distribution of interstitial impurities.

REFERENCES

[1] K. Schulze, "Preparation and Characterization of Ultra-High-Purity Niobium" Journal of Metals, Vol.: 33, Issue: 5, (1981)
[2] K. Schulze, J. Fuß, H. Schultz and S. Hofmann, "Einfluss interstitieller Fremdatome auf den Restwiderstand von reinem Niob" Zeitschrift für Metallkunde, Vol.: 66, Issue: 11, (1976)
[3] J. Fuss, K. Schulze and H. Schultz, "Deviations from Matthiesens Rule in Nitrogen Doped Niobium" J. Phys. F.: Metal Phys.8 (3), p.: 497-743, (1978)
[4] R. Casperson, R. Pohl, H.-M. Thomas, "Berichtsband der DGZFP 68" 735–742 (1999). Available from <http://www.ndt.net/article/v04n08/casperson/casperson.htm> (in German).
[5] U. F. Cocks, C. N. Tome, H. R. Wenk, "Texture and Anisotropy" Cambridge University Press, (2005)
[6] E. Bruder, Unpublished research results, TU-Darmstadt, (2010)
[7] H. Jiang, T.R. Bieler, C. Compton, T.L. Grimm, "Cold rolling evolution in high purity niobium using a tapered wedge specimen", Physica C, Vol.: 441, Issue: 1-2, p.: 118-121, (2006)